

INDC

INTERNATIONAL NUCLEAR DATA COMMITTEE

MEASUREMENT OF PROMPT NEUTRON SPECTRA FOR ^{233}U , ^{235}U AND ^{239}Pu
THERMAL-NEUTRON-INDUCED FISSION IN THE 0.01-5 MeV ENERGY
REGION AND FOR ^{252}Cf SPONTANEOUS FISSION
IN THE 0.01-10 MeV REGION

B.I. Starostov, A.F. Semenov, V.N. Nefedov
V.I. Lenin Scientific Research Institute for Atomic Reactors

Translated by the IAEA

June 1981

Reproduced by the IAEA in Austria

NIIAR P-22(356)

V.I. Lenin Scientific Research Institute for Atomic Reactors

MEASUREMENT OF PROMPT NEUTRON SPECTRA FOR ^{233}U , ^{235}U AND ^{239}Pu
THERMAL-NEUTRON-INDUCED FISSION IN THE 0.01-5 MeV ENERGY
REGION AND FOR ^{252}Cf SPONTANEOUS FISSION
IN THE 0.01-10 MeV REGION

B.I. Starostov, A.F. Semenov, V.N. Nefedov

Nuclear Physics

Dimitrovgrad - 1978

Table of Content

| | <u>Page</u> |
|---|-------------|
| Abstract | |
| Introduction | 1 |
| Method, Electronic Equipment, Detectors and Measurement Geometry | 2 |
| Measurement Procedures | 4 |
| Processing of the Measurements | 5 |
| Results from the Measurement of the Prompt Neutron Spectrum for ^{253}Cf Spontaneous Fission | 6 |
| Results from the Measurement of Prompt Neutron Spectra for $^{233}\text{U} + n_{\text{T}}$, $^{235}\text{U} + n_{\text{T}}$ and $^{239}\text{Pu} + n_{\text{T}}$ Fission | 8 |
| Discussion of the Results | 9 |
| Conclusions | 10 |
| References | 32 |

ABSTRACT

The authors give the results of measurements of prompt neutron spectra for ^{233}U , ^{235}U and ^{239}Pu thermal-neutron-induced fission in the 0.01-5 MeV region, and for ^{252}Cf spontaneous fission in the 0.01-10 MeV region.

The spectra exceed the Maxwellian distributions in the region $E < 0.4$ MeV. The average excess is ~20% over the range $E = 0.05-0.15$ MeV and 5%-7% over the range 0.15-0.4 MeV for the ^{252}Cf fission neutron spectrum.

The spectra were analysed after they and the corresponding Maxwellian distributions had been normalized to the same area. In the 0.05-0.22 MeV region the $^{235}\text{U} + n_{\text{T}}$ fission neutron yield exceeds the ^{252}Cf and $^{239}\text{Pu} + n_{\text{T}}$ fission neutron yields by ~8% and ~15%, respectively. In the 0.3-1.2 MeV region, the $^{235}\text{U} + n_{\text{T}}$ yield exceeds the $^{239}\text{Pu} + n_{\text{T}}$ yield by 8%. There is no difference in the $^{235}\text{U} + n_{\text{T}}$ and $^{233}\text{U} + n_{\text{T}}$ fission neutron spectra in the 0.05-0.6 MeV region.

1. INTRODUCTION

The measurement of prompt fission neutron spectra is of relevance both to the practical problems of nuclear reactor calculations and to the study of the neutron emission mechanism itself. A considerable amount of experimental data has been accumulated on spectra in the $E > 0.5$ MeV region. It is considered that the spectra in the 0.5-8 MeV region are described by a Maxwellian distribution.

$$n_M(E) = C\sqrt{E} e^{-E/T} \quad (1)$$

Where

C is a constant

E is the neutron energy

T is the nuclear temperature

In reactor calculations it is assumed that the spectra fit distribution (1) throughout the energy range, but this is not an established fact. There are considerable discrepancies in the data published by various authors covering the $E = 0.5-1$ MeV region. At $E < 0.5$ MeV, where measurements are very difficult to perform, the fission neutron spectra for the $^{235}\text{U} + n_T$ and $^{239}\text{Pu} + n_T$ nuclides, which are the main components of nuclear fuel, have not been investigated, nor has the $^{239}\text{Pu} + n_T$ neutron spectrum been studied adequately in the $E = 1-8$ MeV region. There are no data on the $^{233}\text{U} + n_T$ fission neutron spectrum in the $E < 0.8$ MeV region. The prompt neutron spectrum for ^{252}Cf spontaneous fission has been studied in greatest detail. However, the results break down into two groups with mean energies of 2.1 and 2.37 MeV, respectively [1]. Moreover, certain authors have published conflicting results in the $E < 0.5$ MeV region right down to $E = 0.002$ MeV [2-9]. Some data [3-5, 7, 10] show that the spectrum in the $E < 0.5$ MeV region exceeds distribution (1) by 20% on average, whereas others [6, 8, 9] fit distribution (1) at $T = 1.4$ MeV over the wide neutron energy range from 0.01 to 10 MeV. The study of the ^{252}Cf fission neutron spectrum was motivated by the IAEA recommendation that this spectrum should be used as an international standard [11].

2. METHOD, ELECTRONIC EQUIPMENT, DETECTORS AND MEASUREMENT GEOMETRY

We used the time-of-flight method in the nanosecond region (Fig. 1). The time-to-pulse-height converter was described in Ref. [12]. We used ^{235}U -based neutron detectors which are insensitive to gamma rays and whose neutron detection efficiency is known over a wide energy range.

Two types of neutron detector were used. For a first series of measurements, the spectra were determined by means of a gas scintillation-ionization detector (GSDIC) with a layer of 90%-enriched metallic ^{235}U [7]. The detector chamber consisted of stainless steel with a diameter of 110 mm and a height h of 170 mm. The thickness of the chamber walls ℓ was 0.5-0.7 mm. A uranium plate 100 mm in diameter and 0.1 mm thick was attached to the bottom of the chamber. An aluminium ring with a nichrome wire mesh, carrying a voltage of ~ 100 V, was placed 5 mm from the plate. The chamber was filled with xenon at 1 atm. Flashes in the gas were detected by an FEU-36 photomultiplier which transmitted pulses to the time-to-pulse-height converter. Ionization pulses from the $^{235}\text{U} + n_{\text{T}}$ fission fragments were transmitted to a "slow" spectrometer control channel (Fig. 1), so that the background caused by the FEU-36 noise and α particles was substantially reduced. The $^{235}\text{U} + n_{\text{T}}$ fission fragments were detected in the surface layer of the plate with an effective thickness of ~ 2 mg/cm².

For a second series of measurements, we used an ionization chamber (IC) in a current pulse mode [13] as the neutron detector. The chamber consisted of stainless steel with the following dimensions: diameter 140 mm, $h = 50$ mm, $\ell = 1$ mm. Eighteen layers of 90%-enriched uranous-uranic ^{235}U were mounted on nine aluminium substrates measuring 90 mm in diameter. The total amount of ^{235}U was ~ 1.3 g. The chamber was filled with methane, and pulses from the ionization chamber were amplified by two preamplifiers [14]. The $^{235}\text{U} + n_{\text{T}}$ fragments were detected with an efficiency of ~ 80 -90%.

As fission fragment detectors, we used two identical gas scintillation detectors (GSD), one of which had a ^{252}Cf layer whilst the other layers were made up from the other nuclides [15]. The GSD chambers consisted of electro-polished stainless steel cylinders 60 mm in diameter and 170 mm in height. The wall thickness varied from 0.2 mm to 0.5 mm. The chambers were filled with a purified mixture of argon and 10% nitrogen at 1 atm. The flashes were detected by an FEU-30 photomultiplier with a stabilized voltage divider [16]. The fissile nuclide targets were placed perpendicular to the

bottom of the chambers on thin wire frames. The ^{252}Cf layers were mounted on stainless-steel substrates. The uranous and uranic ^{233}U , ^{235}U and ^{239}Pu layers, measuring $38 \times 38 \text{ mm}^2$, were mounted on both sides of aluminium foil ($\sim 1.5 \text{ mg/cm}^2$). Sixteen milligrams of each isotope were used for the first series of measurements and 50 mg for the second series.

The spectra were measured in the thermal neutron beam of the SM-2 reactor. The thermal beam was filtered through quartz ($\sim 16 \text{ cm}$) and shaped by a steel collimator with an aperture of $2 \times 20 \text{ mm}^2$. The fission fragment detector was placed in the beam and the neutron detector in the shielding.

For the first series of measurements compound shielding was used. Tanks measuring $90 \times 90 \times 10 \text{ cm}^3$ and filled with a solution of boric acid in water were arranged around the outside of the shielding. In the cavity formed by the tanks we placed a cylinder containing paraffin and boron carbide. The cylinder had an outside diameter of 55 cm and an inside diameter of 35 cm and was 50 cm long. A second cylinder ($\ell = 4 \text{ cm}$) containing boron carbide was placed inside the first cylinder. The neutron detector was mounted along its axis. For the second series of measurements, very simple shielding was used, consisting of paraffin and boron carbide containers forming a cavity with inside dimensions of $80 \times 80 \times 50 \text{ cm}^3$. The wall thickness was 25 cm; there were no front or back walls. The neutron detectors were covered with cadmium ($\ell = 0.5 \text{ mm}$) and 90%-enriched ^{10}B with a thickness of $\sim 0.3 \text{ g/cm}^2$. All the measurements were performed inside additional shielding which consisted of a room measuring $3 \times 3 \times 3 \text{ m}^3$. The neutron background from the reactor was thus reduced as follows:

100 times by covering the detectors with cadmium and ^{10}B ;

20 times by filtering the beam;

6 times by means of the shielding used for the first series of measurements; and

2.5 times by means of the shielding used for the second series;

2-2.5 times in the separate room.

By using detectors which were insensitive to gamma rays, we eliminated the background problems associated with the gamma radiation from the reactor.

3. MEASUREMENT PROCEDURE

In order to determine the fission neutron spectra, we measured the time of flight over various distances L . Although cumbersome, this method is justified because it is sensitive to inaccuracies in the determination of the level of random coincidences and the scattered neutron background. During the first series of measurements, the experiments were performed at $L = 0.104, 0.214$ and 0.295 m. The distances were varied by moving the detector inside the shielding. During the second series, the data were taken at $L = 0.12, 0.214$ and 0.4 m, these distances being changed by moving the neutron detector and shielding as one. At each L setting, measurements were taken over a 24-hour period for 10-20 days for each nuclide.

At the selected pulse discrimination level the fission fragments were detected with an efficiency of $\sim 95\%$ during both series of measurements. The ^{252}Cf fission fragment count rate was $1.2-5.5 \times 10^5$ fragments s^{-1} , depending on the target. For $^{233}\text{U} + n_{\text{T}}$, $^{235}\text{U} + n_{\text{T}}$ and $^{239}\text{Pu} + n_{\text{T}}$, the rates were 1.2×10^5 fragments s^{-1} and 2×10^5 fragments s^{-1} during the first and second series, respectively.

The time resolution was estimated by comparing the theoretical and experimental distributions at $L \sim 4.5$ cm. The resolution was ~ 2.5 ns during the first series and ~ 5.5 ns during the second series. The differential non-linearity of the spectrometer was $\leq 1.5\%$ and the integral non-linearity $\leq 0.5\%$. The zero time setting was determined by calculating the L dependence of the position of the neutron time distribution peak in the analyser channels and then extrapolating this dependence to $L = 0$.

The ^{252}Cf fission neutron spectrum was measured alternately throughout the procedure using the same geometry (accurate to the dimensions of the targets). The FEU-30 and its supply unit were switched from the $^{235}\text{U}/^{239}\text{Pu}$ chamber to the ^{252}Cf gas scintillation detector for this purpose. As an additional check, the ^{252}Cf fission neutron spectrum was also measured both at the beginning and at the end of each series, without the neutron detectors inside the shielding. The reproducibility of the data and the stability of the pulse-height and time characteristics of the detectors and equipment were thus confirmed.

4. PROCESSING OF THE MEASUREMENTS

After the results from the two series of measurements had been summed, six fission neutron time distributions were obtained for $^{233}\text{U} + n_T$, $^{235}\text{U} + n_T$, $^{239}\text{Pu} + n_T$ and ^{252}Cf . The level of random coincidences and the level of random coincidences between neutrons and fragments produced by the various fission events (the background caused by so-called recycled neutrons) were subtracted from all the distributions. All the time spectra, including the ^{252}Cf fission neutron spectra measured without shielding, were then normalized to the same number of recorded neutrons. The time spectra were converted into energy spectra. The efficiency of the neutron detector was assumed to be proportional to the ^{235}U fission cross-sections taken from Ref. [17]. The energy spectra were corrected for resolution in the manner proposed in Ref. [18]. No correction was made for angular anisotropy in the emission of ^{235}U fission fragments in the neutron detector since our calculations showed that this correction would have been $\leq 3\%$ for the first series of measurements and a negligible amount for the second series. Furthermore, the experiments did not show that this correction would have an effect on the neutron spectra.

After the points had been averaged within the limits of the energy resolution, the scattered neutron background was subtracted from the spectra. This background was determined from the difference between the ^{252}Cf fission neutron spectra measurements with and without shielding. The corrections for the scattered neutron background during the second series of measurements are shown in Fig. 2.

After the scattered neutron background had been subtracted, six energy spectra were obtained for each nuclide. From these data we calculated the weighted average values of the spectrum points $\hat{n}_i(E_i)$ and the corresponding weighted average values of the energies \hat{E}_i .

Each spectrum point was assigned a statistical weight:

$$\rho_i = \frac{1}{\left(\frac{\Delta E_i}{E_i}\right) \times \left[\frac{\Delta n_i(E_i)}{n_i(E_i)}\right]^2} \quad (2)$$

Where

ΔE_i is the energy range over which the value $n_i(E_i)$ of point i is averaged;

E_i is the energy corresponding to point i of the spectrum;

$\frac{\Delta n_i(E_i)}{n_i(E_i)}$ is the error in point i of the spectrum, which includes the statistical error allowing for errors in the determination of the random coincidence level and the recycled neutron background, together with the errors relating to the indeterminacy of the ΔL distances and the zero time setting.

On the assumption that the weight ρ_i is uniformly distributed over the range ΔE_i of point i , the contribution to this range of $n(E)$ values by other points was assigned a weight of

$$\rho_j = \delta \rho_k \quad (3)$$

where $\delta = \Delta E_j / \Delta E_k$, i.e. the ratio to the whole range ΔE_k of that fraction of the range ΔE_k of point k in the spectrum, equal to ΔE_j , which overlaps the ΔE_i range of point i . If δ was less than 0.1, the contribution by point k to the weighted average values $\hat{n}_i(E_i)$ and \hat{E}_i of point i of the spectrum was not taken into account. The $\hat{n}_i(E_i)$ and \hat{E}_i values were calculated from the formulae which define them. Each selected $\hat{n}_i(E_i)$ and \hat{E}_i value for the $^{233}\text{U} + n_T$, $^{235}\text{U} + n_T$ and $^{239}\text{Pu} + n_T$ fission neutron spectra was calculated for 5-12 points and for the ^{252}Cf fission neutron spectrum for 10-35 points. Distributions (1) were fitted to the experimental distributions by the least squares method and, together with the experimental points, they were then normalized to a single area, i.e. $\int_0^{\infty} n_M(E) dE = 1$.

5. RESULTS FROM THE MEASUREMENT OF THE PROMPT NEUTRON SPECTRUM FOR ^{252}Cf SPONTANEOUS FISSION

As was shown in Section 4 above, we need to know the ^{252}Cf fission neutron spectrum in order to determine the background caused by neutrons scattered in the shielding devices. For the $E < 0.8$ MeV region there are no data which could be used as a basis for the calculations. We therefore devoted particular attention to the spectrum measurements in this region. We varied the design of the detectors, their wall thickness, the gas filling, the targets and their activity level as well as the L values and the time settings of the analyser channel τ_k . We made a systematic investigation

of the background produced by neutrons scattered on the component parts of the neutron and fission fragment detectors. This effect was determined by successively increasing the thickness of the gas scintillation detector (GSD) and ionization chamber (IC) walls by a factor of 4-10 and measuring the corresponding spectra. The true values of the $n(E)$ spectrum were found by extrapolating the $n(E) = f(\ell_{\text{GSD}}, \ell_{\text{IC}})$ dependences to zero GSD and IC wall thicknesses. We also investigated the background caused by room- and air-scattered neutrons. For this purpose, we carried out measurements when the neutron flux from the fission fragment detector to the neutron detector was covered by a brass shielding cone 32 cm long. The corrections were made to all the spectrum data.

Let us consider the separate sets of ^{252}Cf fission neutron spectrum measurements. The first set (Fig. 3) includes the data obtained with improved neutron and fission fragment detectors. To detect the fission fragments, we used a gas scintillation detector in which the length of the chamber was extended to 27 cm and the wall thickness increased from 0.1 to 0.5 mm. The ^{252}Cf layer was applied to a gold foil of $\sim 100 \mu\text{g}/\text{cm}^2$. As a neutron detector we used an aluminium ionization chamber of diameter 160 mm, $h = 150$ mm and $\ell = 0.8$ mm. Thirty-two layers of uranous-uranic ^{235}U ($\emptyset 85$ mm), altogether containing ~ 3.1 g of ^{235}U [19], were applied to 17 Duralumin substrates 0.05 mm thick and 100 mm in diameter. The ionization chamber was filled with methane. We used two preamplifiers connected in the way described in Ref. [19]. The time resolution of the spectrometer was ~ 5.5 ns. For $L = 0.124$ m, the correction for the scattered neutron background was $\sim 15\%$ at $E < 0.05$ MeV and $\sim 2\%$ at 0.06-0.2 MeV. For $L = 0.214$ m, the background caused by neutrons scattered on the walls of the ionization chamber and gas scintillation detector exceeded the spectrum only in the 0.3-0.8 MeV region, and the correction was $\sim 1.3\%$. For $L = 0.4$ m, the scattered neutron background caused no distortion in the 0.07-0.8 MeV region. The background caused by air-scattered neutrons was $\leq 1.8\%$ of the total number of detected neutrons at $L = 0.4$ m: in a first approximation, this background was found to have an equilibrium distribution over the time scale. The background caused by room-scattered neutrons was reliably distinguished from the true spectrum for all L values < 0.4 m.

The second set of data (Fig. 4) included measurements performed using the improved ionization chamber but with a miniature ionization chamber instead of the gas scintillation fission fragment detector. The ^{252}Cf layer was applied to a stainless steel substrate of $\ell = 0.1$ mm.

The third set of data included measurements taken with the detectors used for the first series of measurements [7]. In this case (Fig. 5), the background caused by neutrons scattered on the detectors was observed at $L = 0.104$ m. The maximum correction for this background was ~40% in the $E < 0.03$ MeV region.

The weighted average spectrum values obtained from the three sets of measurements are in agreement despite the very considerable differences in the measurement conditions (Fig. 6). All the data were therefore used to calculate the final $\hat{n}_i(E_i)$ and \hat{E}_i values. From the resulting ^{252}Cf fission neutron spectrum (Fig. 7), we determined the corrections for the background caused by neutrons scattered in the shielding systems used in the first and second series of measurements.

Distribution (1) was fitted by the least squares method to the ^{252}Cf fission neutron spectrum over the range 0.7-5 MeV. We found that $T = 1.43 \pm 0.02$ MeV. For $T = 1.43$ MeV, the spectrum exceeds distribution (1) by ~20% and 5%-7% in the 0.05-0.15 and 0.15-0.4 MeV regions, respectively.

6. RESULTS FROM THE MEASUREMENT OF PROMPT NEUTRON SPECTRA FOR $^{233}\text{U} + n_T$, $^{235}\text{U} + n_T$ AND $^{239}\text{Pu} + n_T$ FISSION

The $^{233}\text{U} + n_T$, $^{235}\text{U} + n_T$ and $^{239}\text{Pu} + n_T$ fission neutron spectra are considerably distorted by the scattered neutron background (Fig. 2). We therefore had to ascertain to what extent an approximated version of the same energy dependence for the scattered neutron background could be applied to all the fission neutron spectra. This problem was solved in three ways. Firstly, we performed two substantially differing series of measurements. For the first series, the correction for the scattered neutron background was 2-4 times greater than for the second series. Secondly, during both series the measurements were carried out at different L values, so that within the same energy region the corrections differed by several factors. Thirdly, when the $^{235}\text{U} + n_T$ fission spectrum was measured, the shielding system used for the second series of measurements was specially modified in order to increase the scattered neutron background by approximately a factor of 2 (measurements at $L = 0.214^*$ m in Fig. 8). The scattered neutron background must obviously be somewhat different for, e.g. ^{252}Cf and $^{235}\text{U} + n_T$ since the shape of the fission neutron spectra for these isotopes is different. By varying the value and spectrum of the scattered neutron background, we assumed that we would obtain different final results. However, when we compared the data in each series and also the results

obtained from the first and second series, we found that, within the accuracy limits of our measurements (3%-5%), there were no substantial differences in the spectra over a wide energy range (0.04-1.2 MeV) (Figs 8-13). A comparison of the data from the second series for $^{235}\text{U} + n_{\text{T}}$, which were obtained at $L = 0.214$ m and $L = 0.214^*$ m (Fig. 11), revealed that the spectra match one another to within 3%-5% in the 0.06-0.7 MeV region. All the results on the $^{239}\text{Pu} + n_{\text{T}}$ fission neutron spectrum are also in agreement (Fig. 12). Consequently, when the above approximation is used to process the spectra, the upper error limit appears to be less than 5% in the $E < 0.2$ MeV region and less than 3% in the 0.2-1.2 MeV region.

The T parameters for distribution (1) were calculated in terms of the $\hat{n}_i(E_i)$ and \hat{E}_i values. In the 0.5-4 MeV region, the $^{235}\text{U} + n_{\text{T}}$ neutron spectrum fits distribution (1) at $T = 1.31 \pm 0.04$ MeV, but in the 0.05-0.15 MeV and 0.15-0.3 MeV regions the $\hat{n}_i(E_i)$ values exceed the $n_{\text{M}}(E)$ values by on average $\sim 30\%$ and $\sim 10\%$, respectively. The $^{239}\text{Pu} + n_{\text{T}}$ fission neutron spectrum fits distribution (1) at $T = 1.40 \pm 0.04$ MeV, but in the 0.3-1.2 MeV region the $\hat{n}_i(E_i)$ values are 5%-7% less than the corresponding $n_{\text{M}}(E)$ values. The $^{233}\text{U} + n_{\text{T}}$ fission neutron spectrum is normalized to distribution (1) at $T = 1.32$ MeV [20,21]. In Fig. 14 and Tables 1-4, the measurement errors are expressed as the confidence limits for confidence level $\beta = 0.95$. No allowance was made for the error in determining the efficiency of the neutron detector ($\sim 3\%$).

7. DISCUSSION OF THE RESULTS

In the $E < 0.4$ MeV region the data on the ^{252}Cf fission neutron spectrum confirm the findings reported in Refs [3-5, 10], which concluded that the spectrum exceeded distribution (1). Figure 15 shows not only the results from the present paper but also the ^{252}Cf fission neutron spectrum from Refs [8, 9], together with the spectrum plotted according to the formula proposed in Refs [10, 22]. This formula may be used to describe the spectrum in the $E < 1$ MeV region [10, 22]. In the present paper the calculations are extended to cover the 0.01-10 MeV region using the parameters $T = 1.43$ and 1.6 MeV. At $T = 1.6$ MeV, the spectrum may be described by the distribution proposed in Refs [10, 22] over the 1-8 MeV range, but at $E < 1$ MeV the spectrum deviates considerably from the calculated values.

The $n(E)$ values for the ^{252}Cf fission neutron spectrum in the 0.3-0.8 MeV region are 10%-15% less than those published in Refs [8, 9]. At $E < 0.05$ MeV, the data in Ref. [23] are overestimated because no allowance was made for the background caused by the neutrons scattered on the walls of the gas scintillation-ionization detector (GSDIC) and ionization chamber.

It is convenient to take the analysis of the results a stage further and study the ratios of the spectra and of distributions (1) since the $^{233}\text{U} + n_T$, $^{235}\text{U} + n_T$ and $^{239}\text{Pu} + n_T$ neutron spectra were measured under the same background conditions and using the same geometry. The ratio $n(E)_U/n(E)_{Pu}$ at $E = 0.05-0.22$ MeV is 1.24 on average, and the ratio $n_M(E)_U/n_M(E)_{Pu} = 1.065$ if $T_U = 1.31$ MeV and $T_{Pu} = 1.38$ MeV (Fig. 16). In this case the $^{235}\text{U} + n_T$ fission neutron yield exceeds the $^{239}\text{Pu} + n_T$ neutron yield by 16%. We should point out that the spectra were analysed after distributions (1) had been normalized to a single area, i.e. $\int_0^\infty n_M(E)dE = 1$. Over the 0.2-1.2 MeV range $n(E)_U/n(E)_{Pu} = 1.14$ and $n_M(E)_U/n_M(E)_{Pu} = 1.05$, i.e. the $^{235}\text{U} + n_T$ neutron yield is 8% greater than the $^{239}\text{Pu} + n_T$ fission neutron yield. The authors of Ref. [2] noted that the same applies at $E = 0.2-1$ MeV but gave no explanation. On average, the $n(E)_{^{233}\text{U}}/n(E)_{^{235}\text{U}}$ ratios do not deviate from unity over the 0.05-0.6 MeV range. The $^{235}\text{U} + n_T$ neutron yield is ~8% more and ~7% less than the ^{252}Cf fission neutron yield in the 0.05-0.22 MeV and 0.3-0.42 MeV regions, respectively. In the 0.42-4.5 MeV region the $n(E)_{^{235}\text{U}}/n(E)_{^{252}\text{Cf}}$ ratios equal the $n_M(E)_U/n_M(E)_{^{252}\text{Cf}}$ ratios. Over the 0.05-1 MeV range, the ^{252}Cf fission neutron yield is 5%-8% more than the $^{239}\text{Pu} + n_T$ neutron yield. This pattern also shows that the spectra deviate from distributions (1).

8. CONCLUSIONS

1. The prompt neutron spectra for $^{233}\text{U} + n_T$, $^{235}\text{U} + n_T$, $^{239}\text{Pu} + n_T$ and ^{252}Cf fission were measured on one and the same device over the 0.01-5 MeV and 0.01-10 MeV ranges, respectively.
2. The $^{233}\text{U} + n_T$, $^{235}\text{U} + n_T$ and ^{252}Cf fission neutron spectra are shown to exceed distributions (1) in the 0.05-0.3 MeV region. Additional experiments showed that this difference cannot be attributed to the effect of the scattered neutron background on the spectra.
3. Apart from the differences in the spectra apparent as a result of describing them by distributions (1), the $^{235}\text{U} + n_T$ fission neutron yield is significantly higher than the $^{239}\text{Pu} + n_T$ fission neutron yield in the 0.2-1.2 MeV region.

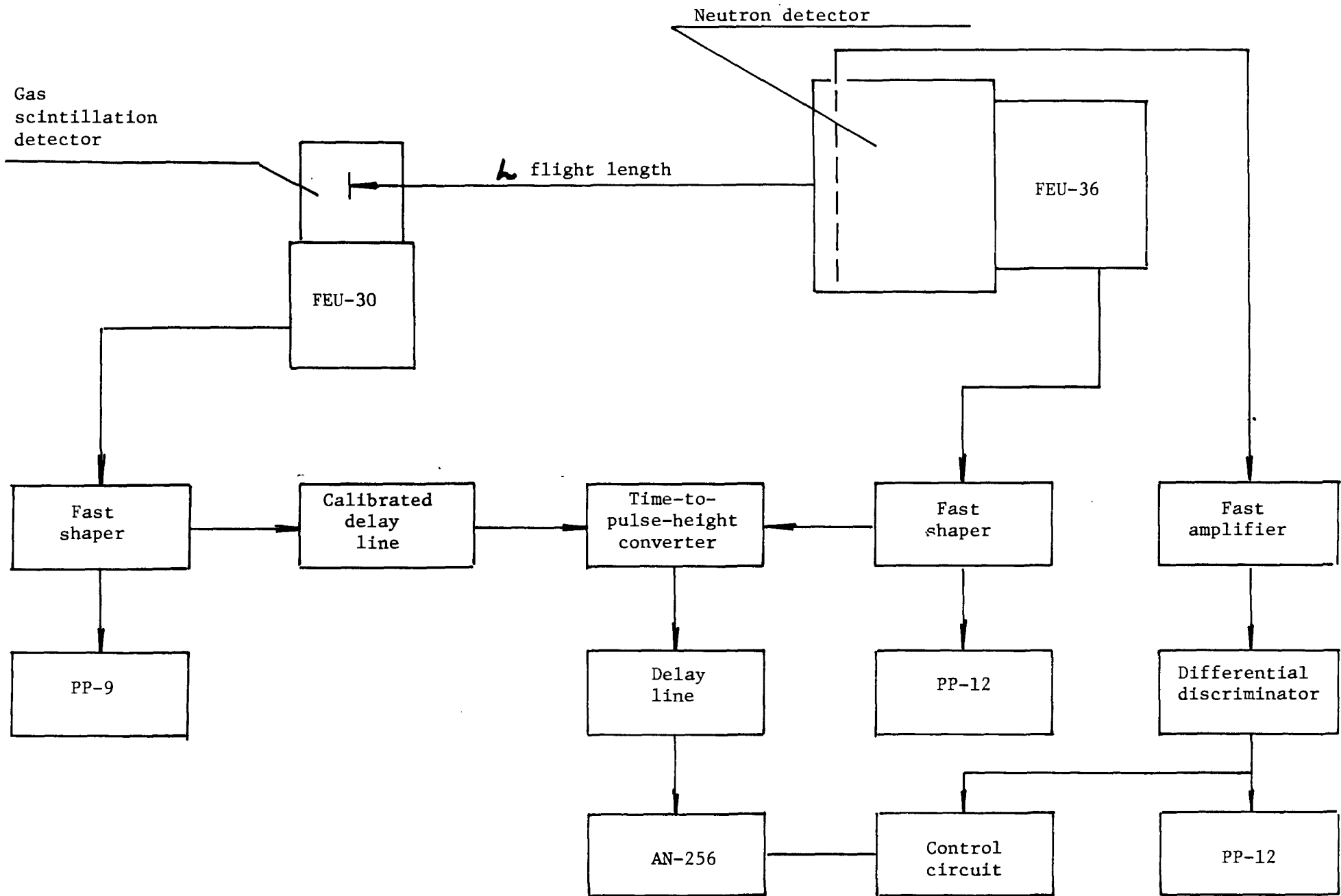


Fig. 1 Simplified block diagram of the electronic equipment

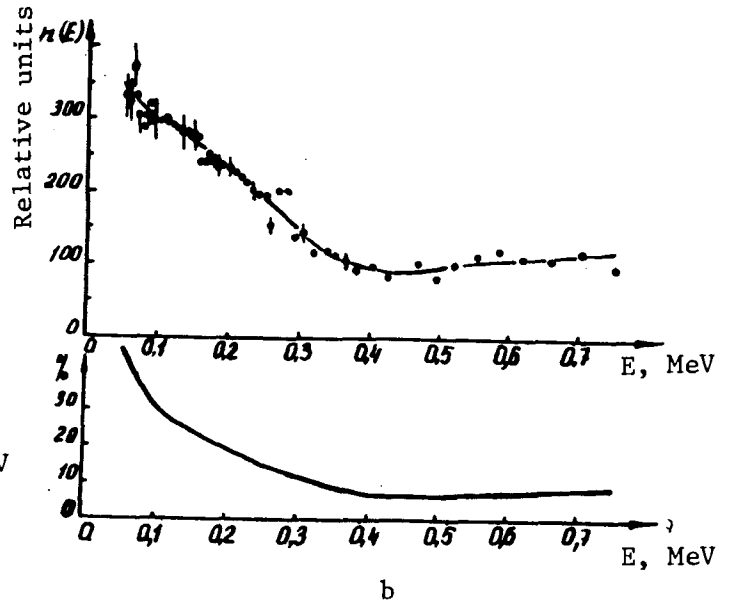
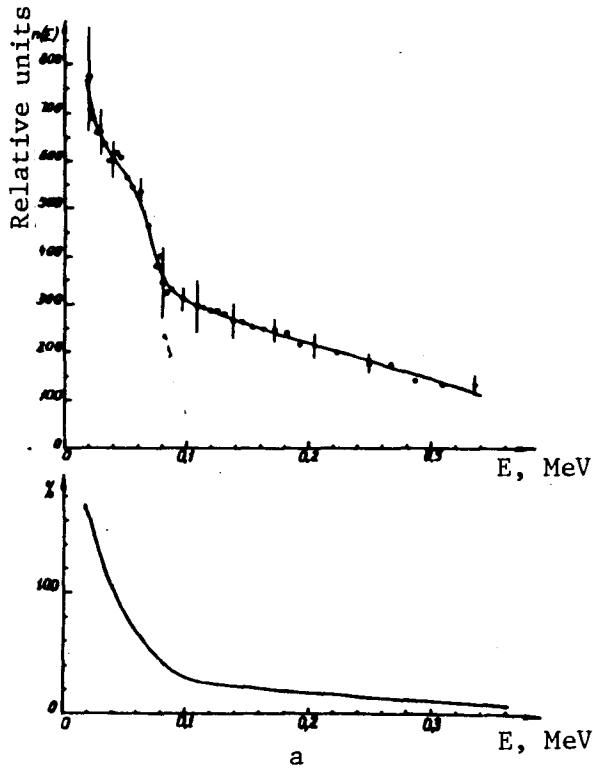
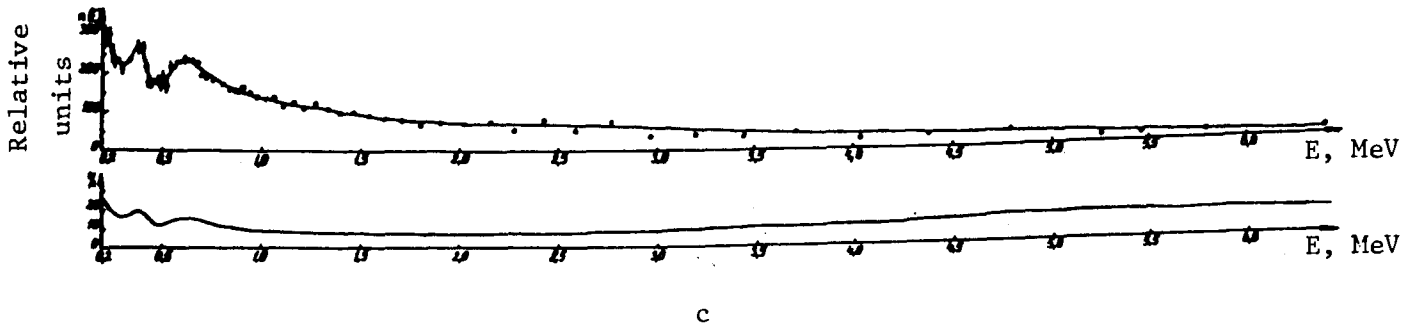


Fig. 2. Scattered neutron background corrections during the second series of measurements.
(a) - $L = 0.12$ m,
(b) - $L = 0.214$ m,
(c) - $L = 0.4$ m.



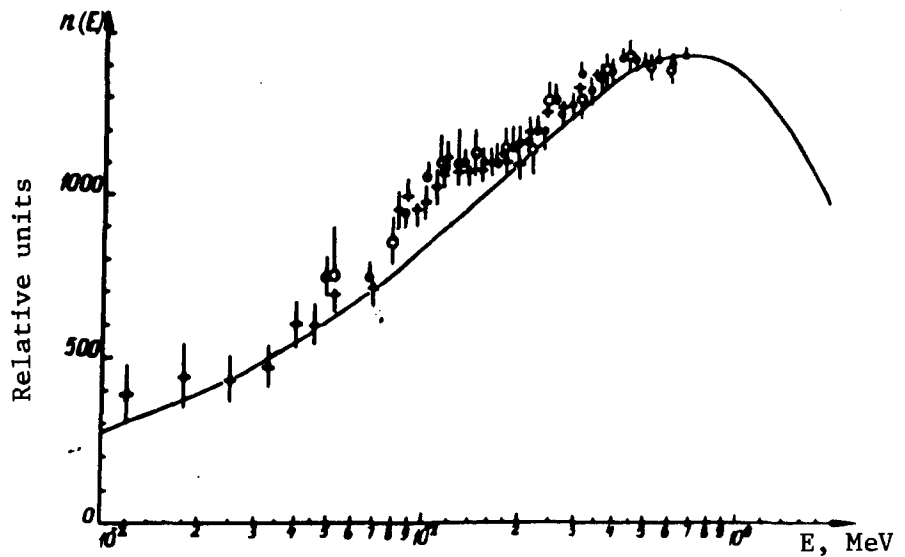


Fig. 3. Prompt neutron energy spectrum for ^{252}Cf spontaneous fission.
 ○ - $L = 0.124$ m, $\tau_k = 0.984$ ns, $n_{\text{fission}} = 2.1 \times 10^5 \text{ s}^{-1}$;
 ● - $L = 0.214$ m,
 ■ - $L = 0.4$ m.
 Distribution (1) = 1.428 MeV

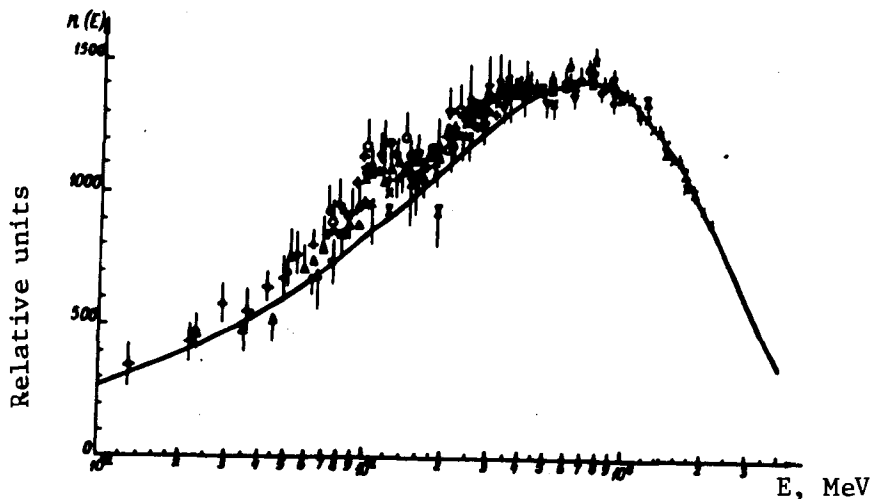


Fig. 4. ^{252}Cf prompt fission neutron energy spectrum
 I $L = 0.147$ m, $n_{\text{fission}} = 0.75 \times 10^5 \text{ s}^{-1}$, $\epsilon_u = 30\%$, substrate $l = 0.1$ mm;
 II $L = 0.147$ m, $n_{\text{fission}} = 2.52 \times 10^5 \text{ s}^{-1}$, $\epsilon_u = 30\%$; III $L = 0.247$ m, $n_{\text{fission}} = 2.52 \times 10^5 \text{ s}^{-1}$, $\epsilon_u = 30\%$, substrate $l = 0.2$ mm; IV $L = 0.247$ m, $n_{\text{fission}} = 2.52 \times 10^5 \text{ s}^{-1}$, $\epsilon_u = 80\%$; V $L = 0.247$ m, $n_{\text{fission}} = 0.75 \times 10^5 \text{ s}^{-1}$, $\epsilon_u = 30\%$; VI $L = 0.497$ m, $n_{\text{fission}} = 2.52 \times 10^5 \text{ s}^{-1}$, $\epsilon_u = 80\%$; VII $L = 0.497$ m, $n_{\text{fission}} = 2.52 \times 10^5 \text{ s}^{-1}$, $\epsilon_u = 30\%$.

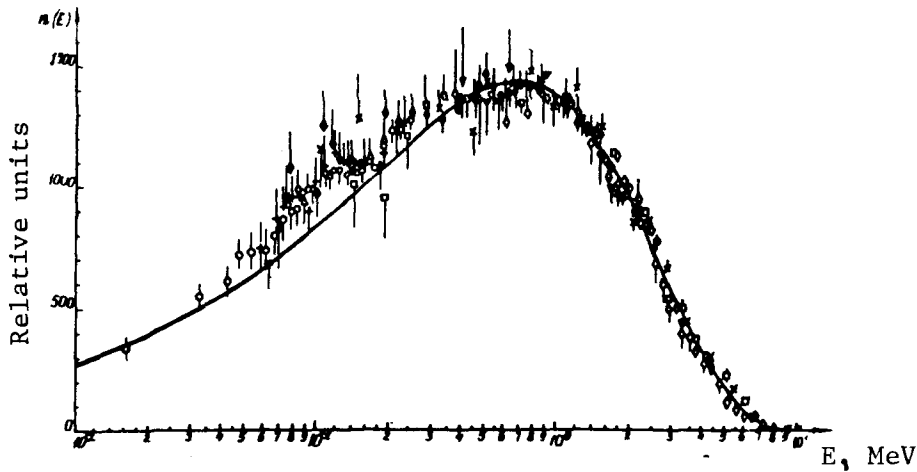


Fig. 5. Prompt neutron energy spectrum for ^{252}Cf spontaneous fission.

\square $L = 0.104$ m, $n_{\text{fission}} = 3.8 \times 10^5 \text{ s}^{-1}$, $\tau_k = 0.68$ ns; \square $L = 0.1$ m,
 $n_{\text{fission}} = 1.2 \times 10^5 \text{ s}^{-1}$, $\tau_k = 0.95$ ns, [7]; \times $L = 0.25$ m [7];
 \square $L = 0.25$ m, $n_{\text{fission}} = 5.5 \times 10^5 \text{ s}^{-1}$, $\tau_k = 0.632$ ns; \blacklozenge $L = 0.214$,
 $n_{\text{fission}} = 3.8 \times 10^5 \text{ s}^{-1}$, $\tau_k = 0.68$ ns; \blacktriangledown $L = 0.5$ m [7]; \blacktriangle $L = 0.131$ m,
 $n_{\text{fission}} = 5.5 \times 10^5 \text{ s}^{-1}$, $\tau_k = 0.632$ ns; \blacklozenge $L = 0.5$ m, n_{fission}
 $= 5.5 \times 10^5 \text{ s}^{-1}$, $\tau_k = 0.632$ ns.

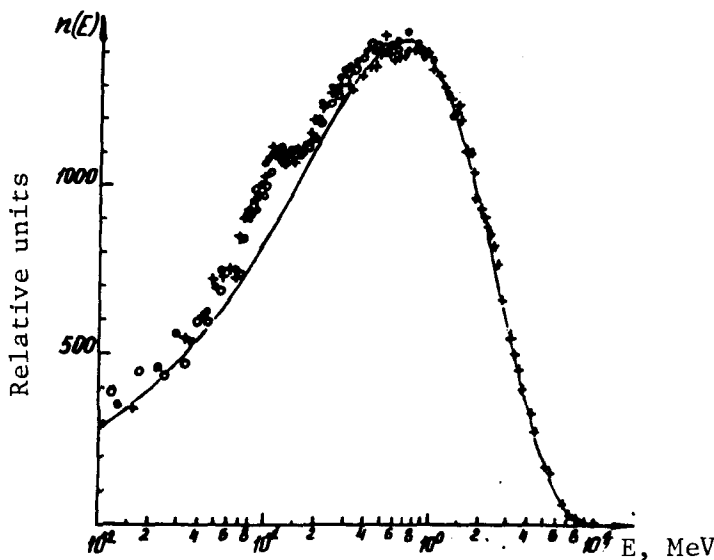


Fig. 6. Prompt neutron energy spectrum for ^{252}Cf spontaneous fission.

\bullet - weighted averages derived from neutron and fission fragment measurements with ionization chambers (IC);
 $+$ - weighted averages derived from measurements with the gas scintillation fission-fragment detector (GSD) and the gas scintillation-ionization (GSDIC) neutron detector;
 \circ - weighted averages derived from measurements with the GSD ($l = 27$ cm) and IC neutron detectors.

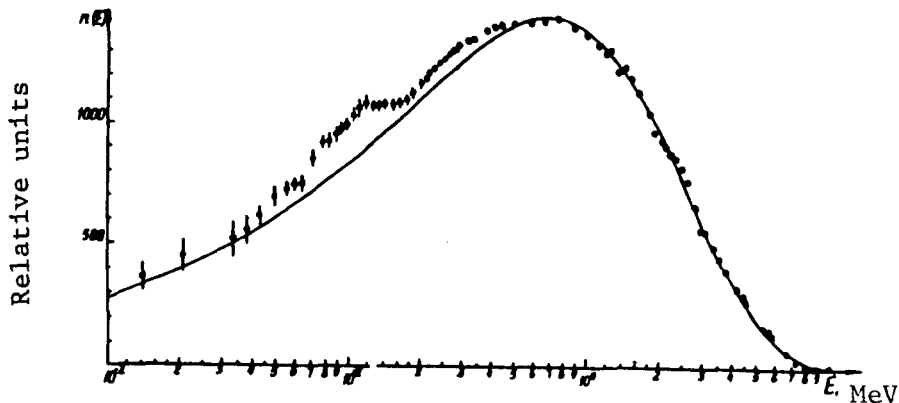


Fig. 7. Weighted averages for the ^{252}Cf fission neutron spectrum, based on all data.

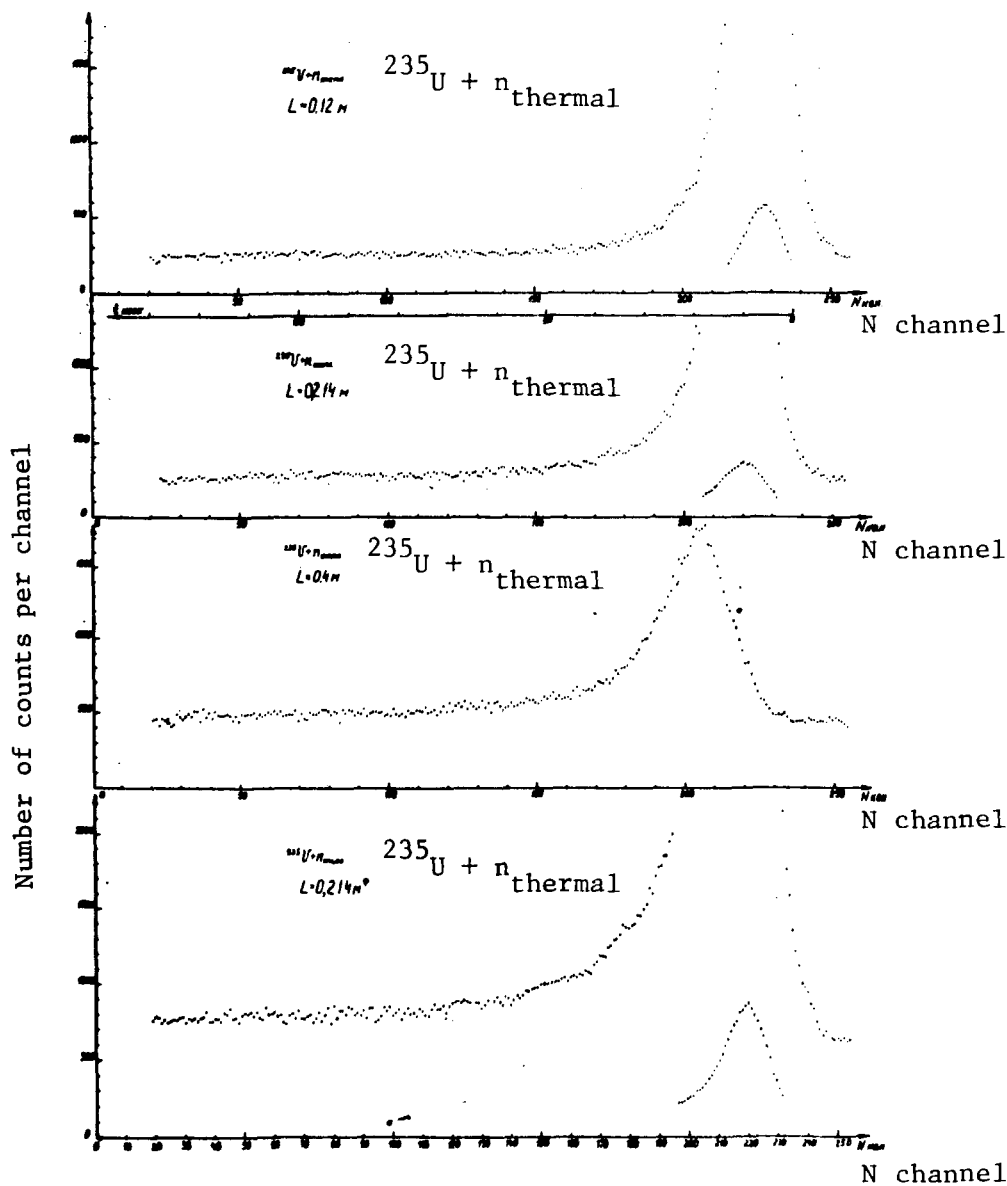


Fig. 8. Prompt fission neutron time spectra for $^{235}\text{U} + n_T$. Second series of measurements: $L = 0.214 \cdot m$, measurements performed with an ionization chamber using the geometry adopted for the first series of measurements.

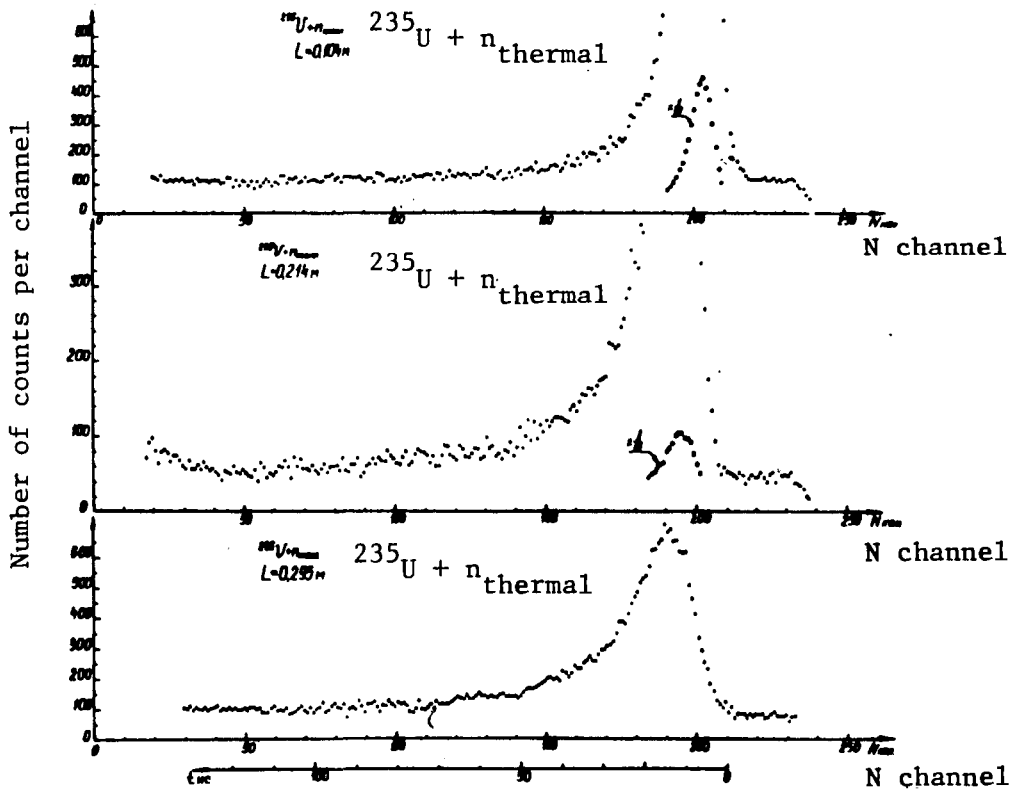


Fig. 9. Prompt fission neutron time spectra for $^{235}\text{U} + n_T$: first series of measurements.

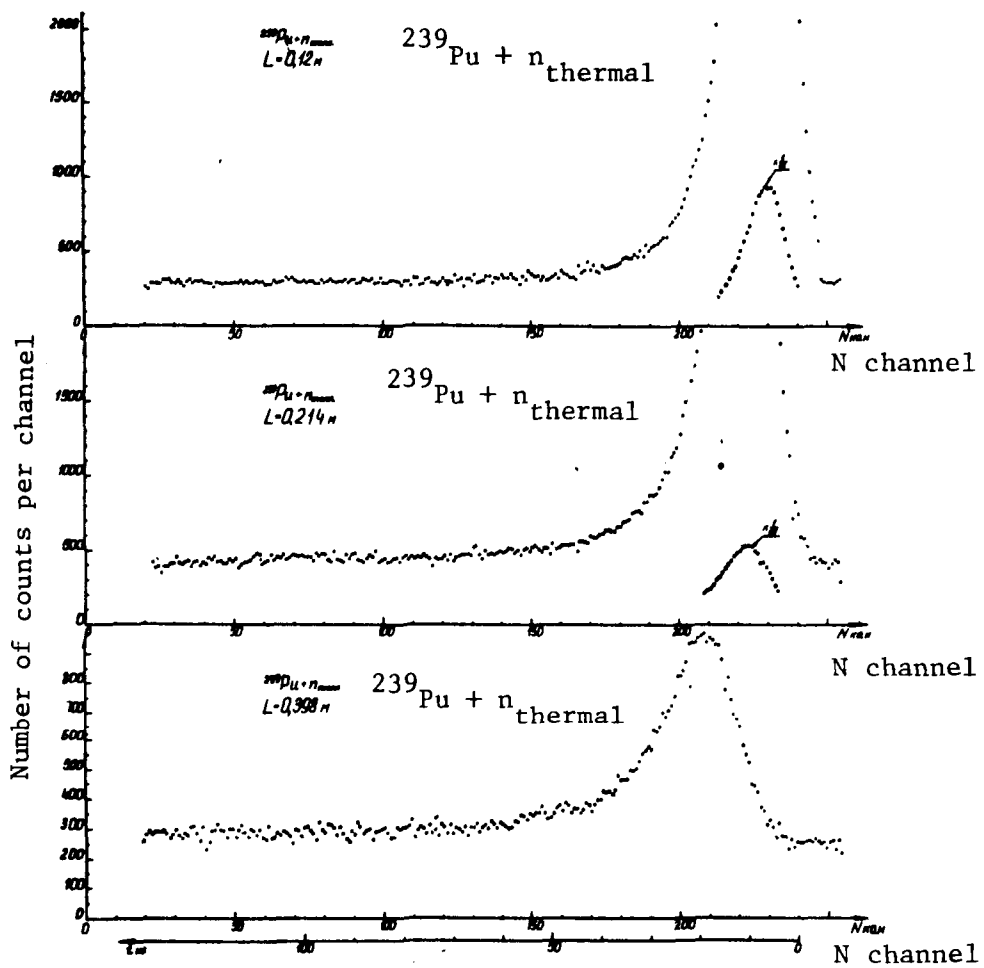


Fig. 10. Prompt fission neutron time spectra for $^{239}\text{Pu} + n_T$: second series of measurements.

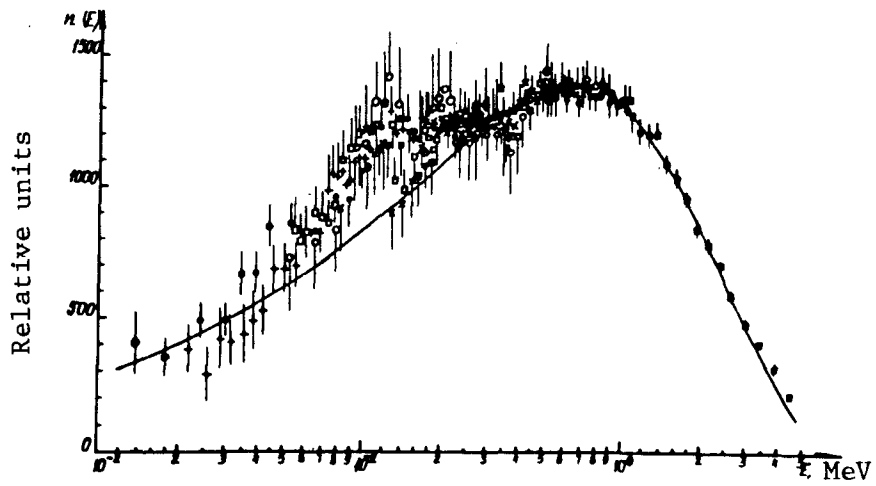


Fig. 11. Prompt fission neutron energy spectrum for $^{235}\text{U} + n_{\text{T}}$.
 First series of measurements: \bullet $L = 0.104$ m,
 \circ $L = 0.214$ m, \blacksquare $L = 0.295$ m.
 Second series of measurements: \boxplus $L = 0.12$ m,
 \boxtimes $L = 0.214$ m, \blacklozenge $L = 0.398$ m, \square $L = 0.214^*$ m.

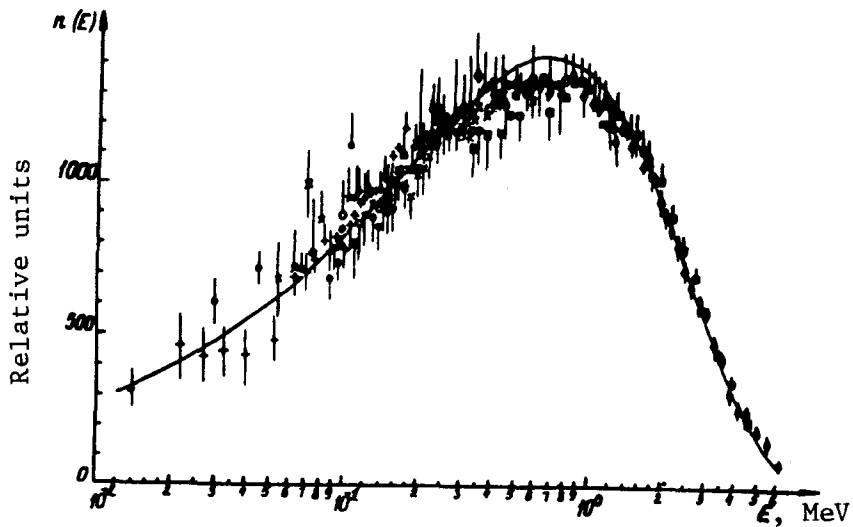


Fig. 12. Prompt fission neutron energy spectrum for $^{239}\text{Pu} + n_{\text{T}}$.
 First series of measurements: \bullet $L = 0.104$ m,
 \circ $L = 0.214$ m, \blacksquare $L = 0.295$ m.
 Second series of measurements: \boxplus $L = 0.124$ m,
 \boxtimes $L = 0.214$ m, \blacklozenge $L = 0.396$ m.

Table 1

Prompt neutron spectrum for ^{252}Cf spontaneous fission

| E, keV | n(E), relative units | $\Delta n(E)/n(E)$, % |
|--------|-------------------------|------------------------|
| 1 | 2 | 3 |
| 14,3 | 0,085 | 12 |
| 21,1 | 0,106 | 9 |
| 33,4 | 0,122 | 8 |
| 36,8 | 0,131 | 7 |
| 43,9 | 0,146 | 6,2 |
| 49,7 | 0,164 | 5,6 |
| 56,2 | 0,172 | 3,9 |
| 65,2 | 0,175 | 4,1 |
| 72,4 | 0,201 | 3,8 |
| 80,4 | 0,216 | 2,9 |
| 84,6 | 0,218 | 2,1 |
| 88,9 | 0,226 | 2,1 |
| 93,8 | 0,230 | 2,3 |
| 98,7 | 0,236 | 2,7 |
| 104,6 | 0,244 | 3,1 |
| 110,6 | 0,251 | 2,5 |
| 117,7 | 0,258 | 1,8 |
| 124,7 | 0,256 | 1,7 |
| 132,7 | 0,254 | 1,7 |
| 141,4 | 0,255 | 1,5 |
| 151,7 | 0,256 | 1,6 |
| 162,1 | 0,257 | 1,1 |
| 174,9 | 0,260 | 1,1 |
| 187,3 | 0,266 | 1,5 |
| 202,7 | 0,278 | 1,9 |
| 208,0 | 0,281 | 1,7 |
| 220,8 | 0,286 | 1,5 |
| 227,5 | 0,289 | 1,5 |
| 244,7 | 0,297 | 1,3 |
| 253,9 | 0,301 | 1,2 |

Table 1, continued

| 1 | 2 | 3 |
|-------|-------|-----|
| 271,3 | 0,304 | 1,2 |
| 281,5 | 0,305 | 1,2 |
| 302,9 | 0,313 | 1,3 |
| 320,5 | 0,318 | 1,2 |
| 352,0 | 0,319 | 1,2 |
| 398,7 | 0,327 | 1,2 |
| 434,9 | 0,325 | 1,5 |
| 481,7 | 0,332 | 1,1 |
| 528,1 | 0,333 | 1,1 |
| 605,4 | 0,332 | 1,1 |
| 681 | 0,336 | 1,1 |
| 781 | 0,339 | 1,5 |
| 803 | 0,331 | 1,2 |
| 1028 | 0,323 | 1,2 |
| 1151 | 0,314 | 1,2 |
| 1231 | 0,307 | 3,1 |
| 1263 | 0,312 | 2,8 |
| 1289 | 0,301 | 2,1 |
| 1370 | 0,286 | 2,1 |
| 1412 | 0,288 | 2,1 |
| 1485 | 0,294 | 1,7 |
| 1562 | 0,282 | 2,1 |
| 1681 | 0,268 | 1,9 |
| 1773 | 0,261 | 1,9 |
| 1845 | 0,246 | 1,6 |
| 1942 | 0,228 | 1,7 |
| 2069 | 0,221 | 1,7 |
| 2152 | 0,214 | 1,6 |
| 2246 | 0,208 | 1,7 |
| 2383 | 0,203 | 1,7 |
| 2532 | 0,194 | 2,5 |
| 2642 | 0,181 | 3,1 |

Table 1, continued

| 1 | 2 | 3 |
|-------|---------|------|
| 2844 | 0,156 | 4,3 |
| 3002 | 0,134 | 4,1 |
| 3113 | 0,132 | 3,1 |
| 3412 | 0,118 | 3,1 |
| 3572 | 0,107 | 2,5 |
| 3784 | 0,094 | 2,5 |
| 4229 | 0,077 | 3,5 |
| 4479 | 0,071 | 4,2 |
| 4544 | 0,066 | 4,1 |
| 5437 | 0,041 | 4,1 |
| 5647 | 0,038 | 4,1 |
| 5815 | 0,034 | 4,1 |
| 6752 | 0,014 | 3,9 |
| 7310 | 0,007 | 3,8 |
| 7918 | 0,0054 | 4,5 |
| 9171 | 0,0012 | 6,6 |
| 10140 | 0,00082 | 12,5 |

Table 2

Prompt neutron spectrum for ^{235}U thermal-neutron-induced fission

| E, keV | n(E), relative units | $\Delta n(E)/n(E)$, % |
|--------|-------------------------|------------------------|
| 1 | 2 | 3 |
| 14,2 | 0,107 | 25 |
| 18,7 | 0,094 | 20 |
| 24,6 | 0,119 | 20 |
| 30,4 | 0,122 | 24 |
| 35,3 | 0,163 | 24 |
| 39,6 | 0,163 | 17 |
| 45,1 | 0,201 | 10 |
| 56,5 | 0,214 | 5,5 |
| 66,6 | 0,230 | 5,5 |
| 79,8 | 0,266 | 5,1 |
| 91,9 | 0,293 | 4,1 |
| 101,4 | 0,307 | 4,1 |
| 114,1 | 0,320 | 3,7 |
| 125,6 | 0,325 | 7,2 |
| 139,0 | 0,302 | 5,6 |
| 155,4 | 0,293 | 4,1 |
| 173,0 | 0,320 | 3,6 |
| 186,3 | 0,330 | 2,9 |
| 194,9 | 0,330 | 3,1 |
| 205,0 | 0,335 | 1,9 |
| 216,0 | 0,335 | 1,9 |
| 234,0 | 0,328 | 1,8 |
| 253,4 | 0,330 | 1,7 |
| 270,0 | 0,332 | 2,7 |
| 282,3 | 0,333 | 1,8 |
| 298,3 | 0,331 | 1,5 |
| 313,8 | 0,333 | 1,5 |
| 331,5 | 0,331 | 3,3 |
| 350,2 | 0,330 | 3,9 |

Table 2, continued

| 1 | 2 | 3 |
|-------|-------|-----|
| 370,6 | 0,326 | 3,3 |
| 393,4 | 0,346 | 2,7 |
| 418,7 | 0,360 | 2,9 |
| 444,3 | 0,363 | 2,1 |
| 474,5 | 0,366 | 2,1 |
| 507,2 | 0,370 | 1,7 |
| 540,8 | 0,366 | 1,5 |
| 582,2 | 0,368 | 1,5 |
| 628,6 | 0,370 | 1,6 |
| 678,0 | 0,368 | 1,5 |
| 732,4 | 0,368 | 1,6 |
| 795,5 | 0,367 | 1,5 |
| 845,9 | 0,373 | 1,5 |
| 901 | 0,365 | 2,6 |
| 962 | 0,360 | 2,4 |
| 1034 | 0,358 | 3,9 |
| 1089 | 0,347 | 3,9 |
| 1192 | 0,328 | 4,1 |
| 1287 | 0,325 | 4,1 |
| 1393 | 0,325 | 4,1 |
| 1514 | 0,294 | 4,5 |
| 1651 | 0,280 | 4,8 |
| 1807 | 0,258 | 4,1 |
| 1987 | 0,228 | 4,2 |
| 2195 | 0,212 | 4,3 |
| 2437 | 0,191 | 4,3 |
| 2722 | 0,160 | 4,4 |
| 3060 | 0,130 | 4,4 |
| 3465 | 0,107 | 4,5 |
| 3956 | 0,087 | 4,7 |
| 4560 | 0,059 | 5,5 |

Table 3

Prompt neutron spectrum for ^{239}Pu thermal-neutron-induced fission

| E, keV | n(E), relative units | $\Delta n(E)/n(E)$, % |
|--------|-------------------------|------------------------|
| 1 | 2 | 3 |
| 19,5 | 0,101 | 20 |
| 30,0 | 0,115 | 19 |
| 46,9 | 0,147 | 18 |
| 55,3 | 0,158 | 17 |
| 64,8 | 0,169 | 10 |
| 72,1 | 0,185 | 10 |
| 81,8 | 0,190 | 5,5 |
| 93,0 | 0,191 | 5,5 |
| 102,4 | 0,211 | 5,5 |
| 111,4 | 0,226 | 5,1 |
| 120,8 | 0,229 | 3,7 |
| 131,1 | 0,231 | 3,6 |
| 141,4 | 0,234 | 5,1 |
| 149,8 | 0,242 | 7,4 |
| 155,1 | 0,251 | 6,4 |
| 162,2 | 0,257 | 5,4 |
| 173,9 | 0,258 | 5,1 |
| 185,9 | 0,261 | 6,1 |
| 197,6 | 0,266 | 3,7 |
| 207,4 | 0,274 | 2,7 |
| 220,7 | 0,277 | 3,1 |
| 235,4 | 0,291 | 2,7 |
| 249,5 | 0,294 | 2,3 |
| 263,7 | 0,295 | 3,2 |
| 288,5 | 0,295 | 2,2 |
| 305,7 | 0,292 | 2,1 |
| 320,0 | 0,296 | 2,1 |
| 333,8 | 0,294 | 2,5 |
| 350,0 | 0,304 | 3,2 |
| 374,4 | 0,305 | 4,1 |

Table 3, continued

| 1 | 2 | 3 |
|-------|-------|-----|
| 400,7 | 0,307 | 2,5 |
| 423,5 | 0,315 | 3,1 |
| 443,9 | 0,319 | 5,3 |
| 469,8 | 0,318 | 4,2 |
| 508,8 | 0,317 | 2,7 |
| 551 | 0,321 | 2,5 |
| 586 | 0,324 | 2,8 |
| 634 | 0,324 | 2,5 |
| 688 | 0,319 | 3,4 |
| 749 | 0,321 | 2,2 |
| 799 | 0,325 | 3,3 |
| 844 | 0,324 | 2,2 |
| 968 | 0,316 | 3,6 |
| 1046 | 0,316 | 2,6 |
| 1116 | 0,306 | 3,8 |
| 1189 | 0,298 | 5,0 |
| 1288 | 0,296 | 4,5 |
| 1405 | 0,287 | 3,2 |
| 1524 | 0,283 | 4,1 |
| 1666 | 0,267 | 5,5 |
| 1822 | 0,253 | 6,1 |
| 2003 | 0,230 | 6,1 |
| 2216 | 0,208 | 6,2 |
| 2450 | 0,184 | 7 |
| 2744 | 0,162 | 8 |
| 3085 | 0,141 | 8,5 |
| 3479 | 0,111 | 10 |
| 3997 | 0,076 | 10 |
| 4515 | 0,060 | 10 |

Table 4
Prompt neutron spectrum for ^{233}U thermal-neutron-induced fission

| E, keV | n(E), relative units | $\Delta n(E)/n(E)$, % |
|--------|-------------------------|------------------------|
| 1 | 2 | 3 |
| 18,3 | 0,115 | 30 |
| 25,1 | 0,118 | 28 |
| 30,8 | 0,125 | 25 |
| 43,1 | 0,207 | 20 |
| 57,6 | 0,205 | 11 |
| 67,5 | 0,194 | 16 |
| 82,8 | 0,243 | 16 |
| 97,0 | 0,298 | 6,1 |
| 109,1 | 0,288 | 5,7 |
| 120,0 | 0,287 | 6,8 |
| 133,9 | 0,312 | 5,1 |
| 154,3 | 0,342 | 5,4 |
| 175,7 | 0,342 | 4,1 |
| 199,2 | 0,346 | 4,1 |
| 236,9 | 0,346 | 4,1 |
| 284,3 | 0,349 | 5,0 |
| 341,3 | 0,353 | 4,3 |
| 383,6 | 0,363 | 5,8 |
| 447 | 0,359 | 5,3 |

Table 4, continued

| 1 | 2 | 3 |
|------|-------|-----|
| 493 | 0,369 | 7,8 |
| 537 | 0,359 | 7,3 |
| 568 | 0,369 | 7,3 |
| 737 | 0,366 | 2,5 |
| 849 | 0,361 | 2,6 |
| 964 | 0,363 | 2,6 |
| 1065 | 0,360 | 6,3 |
| 1197 | 0,336 | 6,8 |
| 1295 | 0,312 | 6,4 |
| 1372 | 0,314 | 5,3 |
| 1514 | 0,297 | 6,1 |
| 1651 | 0,278 | 5,8 |
| 1807 | 0,256 | 5,7 |
| 1987 | 0,239 | 5,8 |
| 2195 | 0,219 | 5,8 |
| 2437 | 0,186 | 5,8 |
| 2722 | 0,157 | 6,0 |
| 3060 | 0,140 | 6,5 |
| 3465 | 0,09 | 8,0 |
| 3956 | 0,08 | 10 |
| 4559 | 0,07 | 15 |

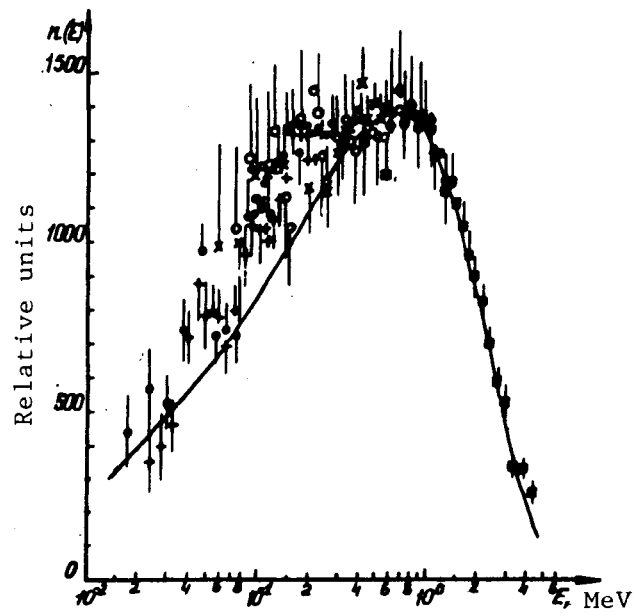


Fig. 13 Prompt fission neutron energy spectrum for $^{233}\text{U} + n_T$

First series of measurements: I $L = 0.104$ m,
 II $L = 0.214$ m, III $L = 0.295$ m.

Second series of measurements: IV $L = 0.124$ m,
 V $L = 0.214$ m, VI $L = 0.396$ m.

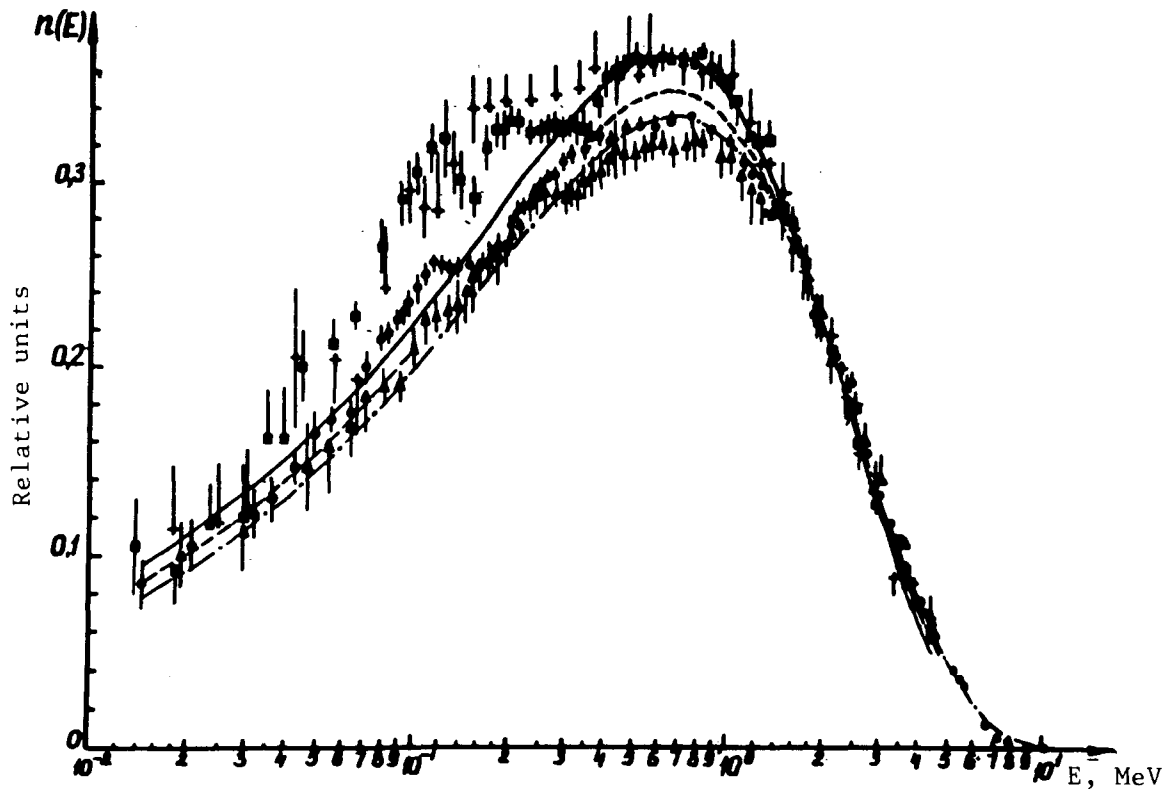


Fig. 14 Prompt fission neutron energy spectra for $^{233}\text{U} + n_{\text{T}}$, $^{235}\text{U} + n_{\text{T}}$, $^{239}\text{Pu} + n_{\text{T}}$ and ^{252}Cf .

I - ^{252}Cf neutron spectrum, I - $^{239}\text{Pu} + n_{\text{T}}$ neutron spectrum,
 I - $^{235}\text{U} + n_{\text{T}}$ neutron spectrum,
 I - $^{233}\text{U} + n_{\text{T}}$ neutron spectrum.

Maxwellian T distribution: — · — T = 1.428 MeV,
 - - - - - T = 1.38 MeV, ————— T = 1.31 MeV.

Weighted average values for $n(E)$ and E .

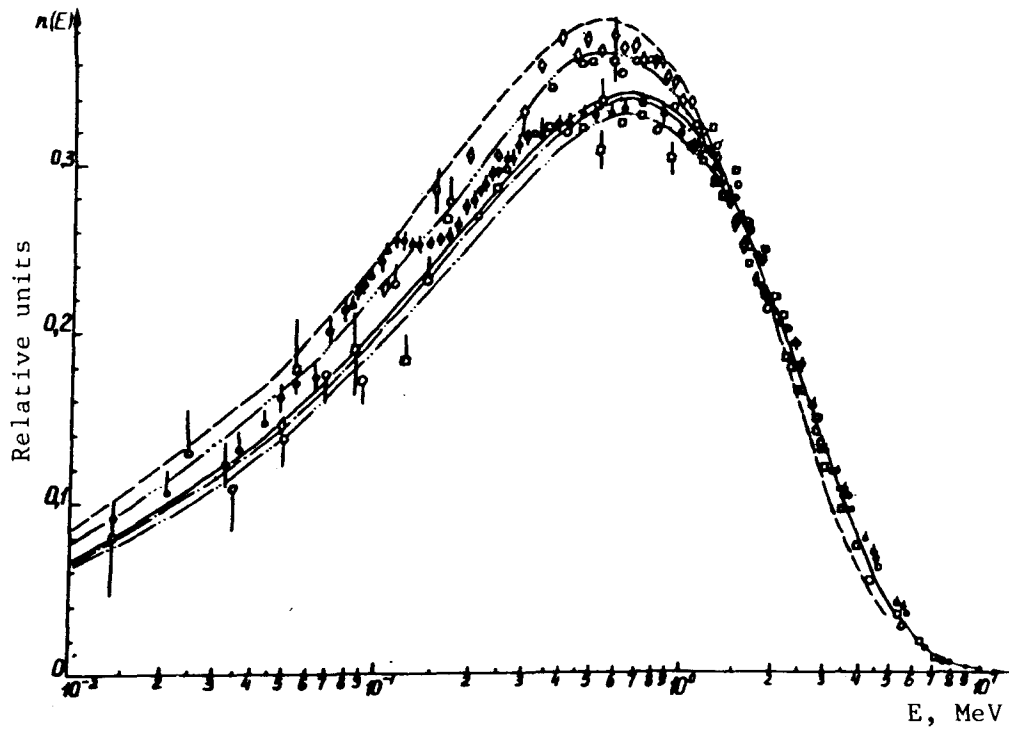


Fig. 15

^{252}Cf prompt fission neutron energy spectrum

$\bar{\Gamma}$ - results from this paper; $\bar{\square}$ - results from Ref. [8]; $\bar{\square}$ - results from Ref. [9].

Distribution (1): ———— $T = 1.406$ MeV;
 - . - . - $T = 1.428$ MeV; - .. - $T = 1.46$ MeV;
 - - - - - and - ... - = spectrum calculated by means of formula in Ref. [10] with $T = 1.43$ MeV and $T = 1.6$ MeV respectively.

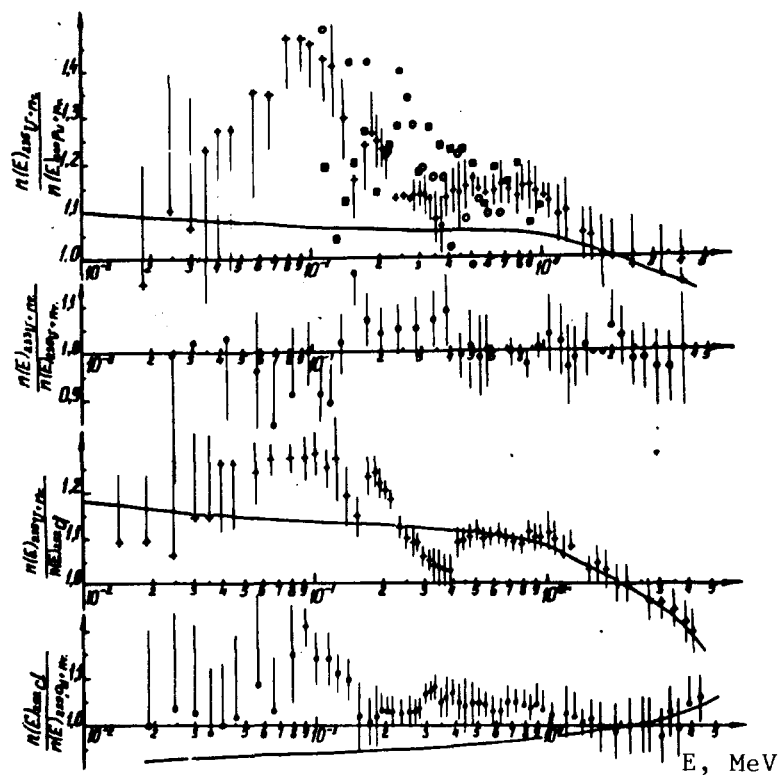


Fig. 16 Ratios of fission neutron spectra and corresponding Maxwellian distributions

$\bar{\Gamma}$ $\bar{\Gamma}$ - results from this paper; \bullet - data from Ref. [2], obtained using a ^3He spectrometer;
 \blacksquare - data from Ref. [2], obtained using a recoil proton spectrometer.

REFERENCES

1. Koster A. Prompt Fission Neutron Spectra, IAEA, Vienna, 1972, p.19-28.
2. Werle H., Bluhm H. Prompt Fission Neutron Spectra, IAEA, Vienna, 1972, p.65-80.
3. Meadows J.W. Phys. Rev., 1967, v.157, p.1076.
4. Zamyatnin V.S., Kroskin N.J., Melnikov A.K., Nefedov V.H. Nuclear data for reactors, IAEA, Vienna, 1972, p.81.
5. Jeki L., Kluge Gy, Laitai A., Dyachenko P., Kuzminov B. Prompt Fission Neutron Spectra, IAEA, Vienna, 1972, p.81-87.
6. BLINOV, M.V., VITENKO, V.A., KAZARINOV, N.M., et al., "Izmerenie spektra nejtronov deleniya ^{252}Cf v oblasti ehnergij 0.02-0.2 MehV" ("Measurement of the ^{252}Cf fission neutron spectrum in the 0.02-0.2 MeV region), in Nejtronnaya fizika, 4, Obninsk TsNIIatominform (1974) 138.
7. NEFREDOV, V.N., STAROSTOV, B.I., SEMENOV, A.F. "Spektr nejtronov deleniya ^{252}Cf v diapazone 0.01-10 MehV" (" ^{252}Cf fission neutron spectrum in the 0.01-10 MeV region"), in Metrologiya nejtronnogo izlucheniya na reaktorakh i uskoritelyakh, 2, Moscow TsNIIatominform (1974) 139.
8. BATENKOV, O.I., BLINOV, M.V., VITENKO, V.A., et al., "Izmerenie spektra nejtronov deleniya ^{252}Cf v oblasti ehnergij 0.02-2.0 MehV" ("Measurement of the ^{252}Cf fission neutron spectrum in the 0.02-2.0 MeV region"), in Nejtronnaya fizika 5, Moscow TsNIIatominform (1976) 114.
9. BLINOV, M.V., VITENKO, V.A., TUZ, V.T., Izmerenie spektra nejtronov spontannogo deleniya ^{252}Cf v shirokom intervale ehnergij 0.01-10 MehV (Measurement of the ^{252}Cf spontaneous fission neutron spectrum over the 0.01-10 MeV range), Nejtronnaya fizika, 3, Moscow TsNIIatominform (1977) 197.

10. D'YACHENKO P.P., SEREGINA, E.A., KUTSAEVA, L.S., et al., O spektre nejtronov spontannogo deleniya ^{252}Cf v oblasti malykh ehnergij (Spectrum of low-energy neutrons from the spontaneous fission of ^{252}Cf) At. Ehnerg. (available in English translation as Soviet Journal of Atomic Energy) 42 1 (1977) 25.
11. Prompt Fission Neutron Spectra, IAEA, Vienna, 1972, p.169.
12. BASOVA, B.G., KACHALIN, V.A., STAROSTOV, B.I., Vremya-amplitudnyj konvertor nanosekundnogo diapazona (Time-amplitude (sic) converter for the nanosecond range) Prib. Tekh. Ehksp. (Available in English translations as Instruments and Experimental Techniques) 4 (1970) 69.
13. Posiler H., Millard I.K., Hill N.W. Nuclear Instruments and Methods, 1972, v.99, p.477.
14. KONONOV, V.N., METLEV, A.A., POLETAEV, E.D., PROKOPETS, Yu.S., Bystrodejstvuyushchaya ionizatsionnaya kamera deleniya (Fast ionization chamber for fission) Prib. Tekh. Ehksp. 6 (1969) 51.
15. KROSHKIN, N.I., KORMUSHKINA, G.A., STAROSTOV, B.I., SHIPILOV, V.I., Gazovye tsintillyatsionnye detektory oskolkov deleniya (Gas scintillation detectors for fission fragments) NIIAP Preprint, P106 Dimitrovgrad (1971).
16. VLASOV, M.K., KANAVETS, V.P., LUZHETSKIJ, N.N., et al., Issledovanie rabotosposobnosti fotoumnozhitel'ej FEU-36 i FEU-30 v usloviyakh vysokikh zagruzok i vybor skhem stabilizatsii pitaniya fotoumnozhitel'ej (Investigation of the efficiency of FEU-36 and FEU-30 photomultipliers under heavy-duty conditions and the choice of photomultiplier supply stabilizing circuits) Prib. Tekh. Ehksp. 2 (1968) 239.
17. ANTSIPOV, G.V., BENDERSKIJ, A.R., KON'SHIN, V.A., et al., "Otsenka yadernykh dannykh ^{235}U v oblasti ehnergij nejtronov 10^{-4} ehV-15 MehV dlya cozdaniya polnogo fajla konstant" ("Evaluation of nuclear data on ^{235}U in the 10^{-4} eV-15 MeV region for the purposes of compiling a complete file of constants") from Voprosy atomnoj nauki i tekhniki, 20 2 (1975) 3.
18. KORNILOV, N.V., Vliyanie razresheniya spektrometra i ehnergeticheskogo razbrosa pervichnogo puchka na formu spektra neuprugo-rasseyannykh nejtronov (Effect of spectrometer resolution and primary-beam energy spread on the shape of the inelastic neutron scattering spectrum) FEI Preprint P276 Obninsk (1971).

19. BOGDZEL', A.A., GRIGOR'EV, Yu.V., DLOUGI, Z., et al., Bystro-dejstvuyushchaya ionizatsionnaya kamera deleniya s radiatorami iz ^{235}U (A high-speed fission ionization chamber with radiators made of ^{235}U) Prib. Tekh. Eksp. 1 (1976) 36.
20. Green L., Mitchel I.A., Steen N.M. Nucl. Sci. Eng. 1973, V.50, p.257.
21. ANDREJCHUK, L.M. KOROSTYLEV, V.A., BASOVA, B.G., et al., "Izmerenie spektrov mgnovennykh nejtronov deleniya ^{233}U , ^{235}U , ^{239}Pu teplovymi nejtronami odnositel'nym i absolyutnym metodami" ("Measurement of prompt neutron spectra for ^{233}U , ^{235}U and ^{239}Pu thermal-neutron-induced fission by relative and absolute methods") in Nejtronnaya fizika, 5 Moscow TsNIIatominform (1976) 120.
22. LAJTAJ, A., KECSKEMETY, J., KLUGE, D., et al., "Spektr mgnovennykh nejtronov deleniya ^{235}U teplovymi nejtronami v diapazone ehnergij ot 0.03 do 1 MehV" ("Prompt neutron spectrum for ^{235}U thermal-neutron-induced fission in the 0.03-1 MeV region") in Nejtronnaya fizika, 3 Moscow TsNIIatominform (1977) 26.
23. NEFEDOV, V.M., STAROSTOV, B.I., SEMENOV, A.F., "Spektry mgnovennykh nejtronov deleniya ^{233}U , ^{235}U , ^{239}Pu , ^{252}Cf " ("Prompt fission neutron spectra for ^{233}U , ^{235}U , ^{239}Pu and ^{252}Cf fission") in Nejtronnaya fizika, 3, Moscow TsNIIatominform (1977) 205.